Program Digest, 2019 IEEE International Ultrasonics Symposium (IUS)
Glasgow, Scotland, October 6-9, 2019

A Miniature 16-element Endoscopic Histotripsy Transducer with Electronically Steerable Focus

Matthew Mallay
Biomedical Engineering
Dalhousie University
Halifax, Canada
matt.mallay@dal.ca

Jeffery Woodacre
Biomedical Engineering
Dalhousie University
Halifax, Canada
jwoodacre@dal.ca

Taha Take
Electrical Engineering
Dalhousie University
Halifax, Canada
th504456@dal.ca

Emily Napier
Electrical Engineering
Dalhousie University
Halifax, Canada
em662159@dal.ca

Sandra Gorgey
Electrical Engineering
Dalhousie University
Halifax, Canada
sn961029@dal.ca

Jeremy Brown
Biomedical Engineering,
Electrical and Computer Engineering
Dalhousie University
Halifax, Canada
j.brown@dal.ca

***Abstract*— A 5 mm by 5 mm 16-element histotripsy transducer was built and tested using a lens bonded to an air-backed 1-3 piezoelectric composite. The transducer was driven by a custom designed 16 channel pulse generator. Both aluminum and methacrylate photopolymer (resin) lens designs were modelled using a COMSOL FEM model. A resin lens was 3D printed and used to fabricate a transducer array with a focus that could be steered over a greater area than the aluminum lens design. The resin lens transducer had a peak negative pressure trend of 5.7 MPa/100 V. The -3 dB focal length and width were 1.94 mm and 0.30 mm. A pulse sequence cycling through 5 foci spaced within a 1.5 mm square was used to ablate ex vivo rat brain tissue through shock scattering cavitation near the surface.**

Keywords—histotripsy, ultrasound, transducer design, ablation

I. Introduction

Histotripsy is a therapeutic ultrasound technique for non-invasively ablating tissue. A focused transducer is used to generate a peak negative pressure low enough to cause cavitation, resulting in precise tissue ablation at the focus without damaging the surrounding tissue [1]. We have proposed that histotripsy transducers have the potential to be useful in minimally invasive neurosurgery, particularly in resecting primary tumors during key-hole procedures. Due to the small size of the access hole, the transducer is limited to an endoscopic form factor.

The size of the cavitated area decreases for higher operating frequencies, meaning the desire for a precise treatment region drives the choice of frequency into the 5+ MHz range. By increasing frequency, there is also an inherent trade-off between precision and ablation size for the single element transducers currently developed in our lab. Regardless of the frequency, these have a fixed focus and must be physically moved cut a desired volume, which limits the utility of such a device in minimally invasive surgical applications. By developing a transducer based on a phased linear array, the elements can be beam steered to move the focus, increasing the ablated region without sacrificing precision, and allowing for the ablation of irregular geometries without moving the device itself.

Several prototypes of a miniature histotripsy transducer have been developed by our lab, including those presented in [2] and [3]. Experiments have been conducted in which the histotripsy transducer and the imaging probe were co-registered. This allowed the target area to be imaged during ablation. Most recently, a 5 mm by 5 mm single channel transducer with a focal length of 5 mm was developed [4]. This transducer was based on a 5 MHz PZT5A composite bonded to an aluminum lens with a Parylene matching layer. The maximum pressure output was at an operating frequency of 6.5 MHz. Free-field cavitation in water was demonstrated using this transducer pulsed with a 570 V peak-to-peak drive voltage using a 15-cycle pulse at 1 kHz pulse repetition frequency (PRF).

In this work we present a histotripsy transducer array in an endoscopic form factor, driven by a multi-channel pulser capable of steering the focus by beamforming the array elements.

II. Methods

A. FEM Model

A Finite Element Method (FEM) model of the array was developed using Comsol Multiphysics. The 1-3 thickness mode piezoelectric composite was modelled using the equations in [5], based on the volume fraction, and properties of the piezoelectric ceramic and epoxy. The Poisson's ratio and loss factor of the epoxy were chosen by fitting the impedance of a piece of bare composite measured in air. An epoxy layer thickness of 40 µm was used between the composite and the lens to fit the electrical impedance and output pressure of the transducer.

The model was set up as a 2D cross section through the center of the transducer as shown in Fig. 1. It was used to test

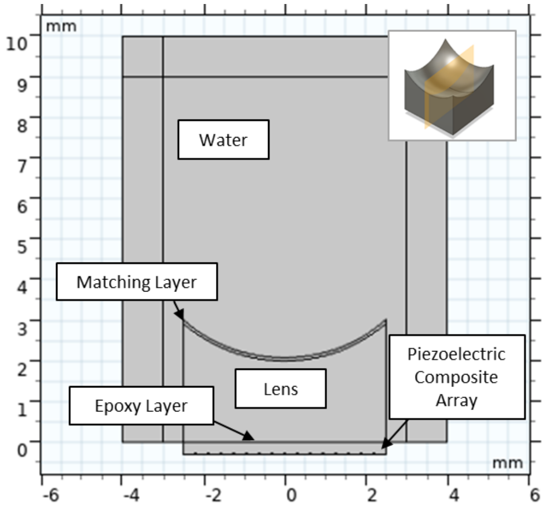

Fig. 1. The geometry of the FEM model annotated to show each component of the transducer. The inset shows the 2D plane through the lens.

the beam forming delays that were calculated in MATLAB using the transit time from each element to the desired focal point. It was also used to simulate changes to the transducer design, particularly the lens. When the aluminum lens with matching layer was replaced by a methacrylate photopolymer (resin) lens with a thinner minimum height there was a slight increase to the peak pressure and a huge improvement in the ability to steer the focus.

The electrical impedance of each array element was calculated by assuming the transducer cross section through the 5 mm depth was constant. Fig. 2 shows electrical impedance from the resin lens transducer model. The elements are well grouped around the minimum impedance of approximately 630 Ω at 5 MHz, except for elements 1 and 16 which have a higher impedance due to being marginally narrower than the other elements.

B. Fabrication

1) Aluminum Lens Transducer

The starting point for this work was to modify the single channel transducer design to have 16 elements which can be pulsed independently. This was accomplished by scratch dicing the electrode from between the pillars of the negative side of the piezo composite. A dicing saw (DAD3220, Disco Hi-Tec, Tokyo, Japan) with a 29 µm blade was used to make the cuts. The full electrode was left on the positive poled side to provide a common ground to the elements.

The back of the aluminum lens was lapped flat and bonded to the positive electrode of the composite using EPOTEK 301 (Epoxy Technology Inc., USA) epoxy. The array elements were connected by wire bonding to a flexible circuit board (flex) oriented perpendicular to the array [6]. A diced section of flex was mounted to the side of the lens. The pads on one side were wire bonded to the array elements and the other side to the main flex PCB. The wire bonds were covered with EPOTEK 301 loaded with alumina. The epoxy layer between the composite and lens was thin enough that the composite could be grounded to the flex through the lens.

2) Resin Lens Transducer

Following the evaluation of the aluminum lens array and an FEM model study, a new transducer design incorporating a lower acoustic impedance lens was fabricated, as shown in Fig. 4. The acoustic lens was 3D printed using Form 2 Clear Resin (Formlabs, Inc., Somerville, MA, USA). A test piece was printed to measure the acoustic properties of the cured resin. The density was 1163 kg/m^3 and the longitudinal speed of sound was 2624 m/s. The curvature of the elliptical lens was adjusted based on sound speed to achieve a focus of 6 mm. The lower sound speed meant the lens curvature couldn't extend to the outer corners of the composite, which reduced the active area by 10%. The focal length and maximum lens height were selected to maintain the same distance from the outer lens surface to the focus as with the aluminum lens.

Using an electrically insulating plastic lens meant the array elements could be oriented on the front face of the transducer eliminating one of the wire bonding steps. Also, the lower acoustic impedance precludes the use of a ¼ wavelength layer to match to water. This significantly reduces the complexity of the fabrication process. The trade-off in this design is that the bandwidth is much lower than the aluminum lens transducer, but this is not detrimental to certain therapeutic applications such as histotripsy.

C. Pulse Generator

A custom 16 channel pulse generator was designed to provide the high voltage pulses to the array. The design was similar to a previously developed single channel pulser [7], but with a silicon carbide NFET to reduce the switching time. The pulser channels were split into groups of eight divided over four PCB cards. Each of the 4-channel pulser boards contained a high voltage 1 Watt DC-DC converter capable of outputting 600 V when unloaded.

The four cards plug into the motherboard to receive supply voltages, as well as a CMOS input waveform for each channel from an FPGA (Kintex XC7K160T-1FBG484C, Xilinx, San

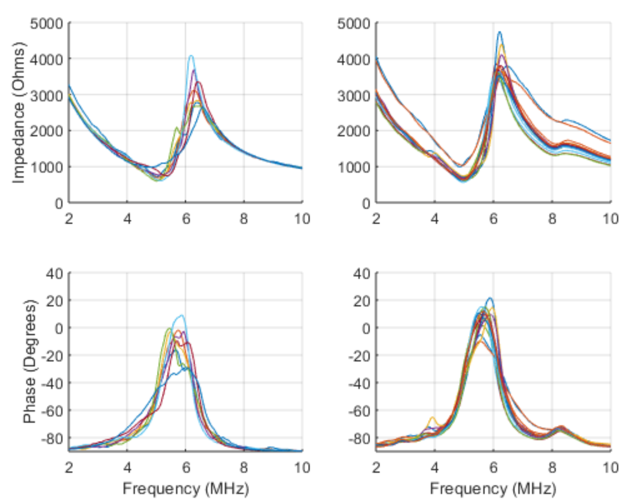

Fig. 2. Impedance magnitude and phase of each array element in the resin lens transducer, from the FEM model (left) and the fabricated array (right).

Jose, Ca). The FPGA was used to implement the appropriate time delays between signals to steer the focus of the array. Each of the pulsers connect to an interposer board which routes the signals through a ZIF connector to a 2 m long cable bundle. A series inductor was used at the output of each pulser channel to cancel out the cable capacitance. This significantly improved the quality of the signal at the array.

III. Results And Discussion

A. Array Characterisation

The peak negative pressure was measured for both array types using a 0.04 mm needle hydrophone (Precision Acoustics Ltd., Dorchester, U.K.) for drive voltages ranging from 10 – 30 V. Eight cycle bursts were used for these measurements, which was more than enough for the hydrophone signal to reach steady state. The aluminum lens transducer had the highest output for a drive frequency of 6.0 MHz; the optimal drive frequency for the resin lens transducer was 5.2 MHz. The linearly interpolated hydrophone sensitivity at these frequencies was 8 mV/MPa and 7.2 mV/MPa, respectively. This shift in frequency appears to be due to the lower elastic modulus at the boundary of the piezoelectric composite as discussed in [3] for increases to epoxy bond line thickness in aluminum lens transducers. The peak negative pressure per volt was linearly extrapolated based on the low voltage measurements. It was found to increase at a rate of 5.9 MPa/100 V for the aluminum lens transducer and 5.7 MPa/100 V for the resin lens transducer.

The model predicted the pressure would increase with the resin lens. There are two possible explanations for this. Small air bubbles were noticed in part of the lens when viewed under a microscope, which would scatter the acoustic waves within the lens. Also, the minimum thickness of the lens was close to the resolution of the 3D printer which resulted in it being slightly deformed.

The single channel aluminum lens transducer presented in [4] produced an output of 8.3 MPa/100 V. The lower array pressure can be attributed to a reduction in the active piezoelectric surface area due to defining the array elements and from the epoxy used to cover the wire bonds.

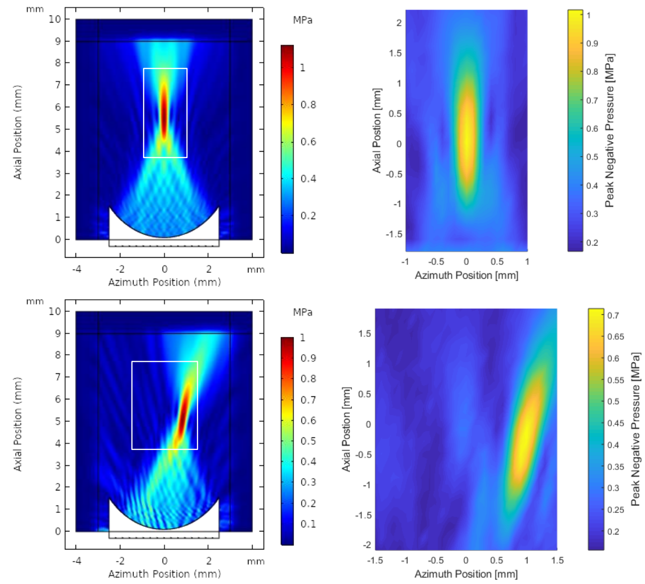

Fig. 3. A comparison of measured radiation patterns (right) to the FEM model (left). The top row shows the transducer focus with no beam forming, the bottom row shows the focus steered 1 mm azimuthally.

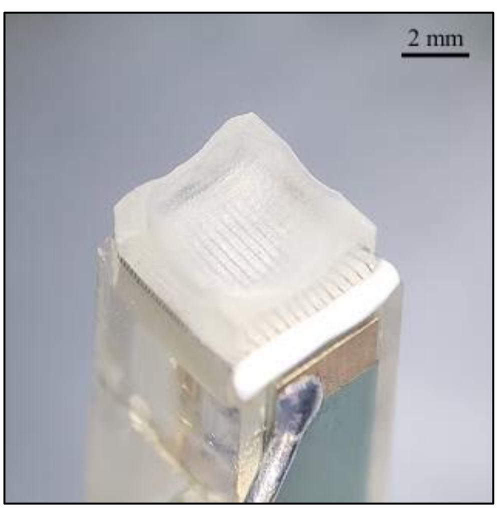

Fig. 4. Finished transducer with the array elements visible through the clear resin lens. A 3D printed case was designed to rigidly mount the composite and flex in the ideal position for wire bonding. The case is hollow to air back the composite, with a push pin used to make the ground connection.

To characterize the focal spot size and beam steering, the transducer was mounted to a 3-axis servo-controlled positioning stage capable of measuring the pressure over a grid of points with high precision. For the aluminum lens array, the nominal focus had a measured axial and azimuthal focal width of 1.24 mm and 0.21 mm respectively, while the model predicted 2.53 mm and 0.27 mm. These measurements were repeated for the resin lens array, which had a measured axial and azimuthal focal width of 1.94 mm and 0.30 mm respectively, while the model predicted 2.23 mm and 0.28 mm. The smallest width of the transducer is modelled, meaning the simulated aperture is less than the average aperture of the transducer. This explains why the measured axial width was lower than predicted.

In Fig. 3, the radiation patterns for the resin lens are compared to the FEM model results for no beam steering, and 1 mm azimuth steering. The array produced a strong focus with a 33% reduction in pressure when steered. By comparison, the aluminum lens transducer could only be azimuthally steered to 0.5 mm before experiencing a similar pressure drop. Steering the focus to 1 mm was not possible with the aluminum lens.

Both arrays designs were able to exceed the extrinsic cavitation threshold using a 250 V drive voltage, by generating a bubble cloud when reflected off a high impedance surface. The PZT 5A composite reached its saturation voltage before it could intrinsically cavitate in water.

B. Ablation

The resin lens array was tested on an ex vivo rat brain with the dura removed. The histotripsy transducer and an imaging array were held in place using independently adjustable fixtures, at an angle of approximately 45 degrees between the forward-

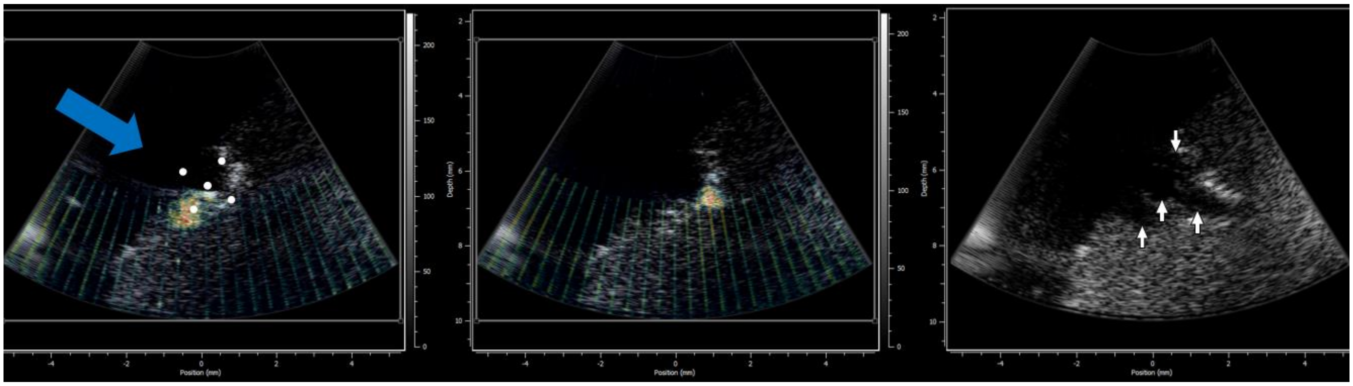

Fig. 5. Images of ablation initiated by steering the focus to five points in a + pattern. The first image shows an arrow indicating the direction of the histotripsy transducer, with dots located at the focal points. The colored spot in the first two images are with power doppler turned on to help visualize the bubble cloud. The third image was captured after the pulse was turned off, where the arrows indicate the ablated regions.

looking axis. They were adjusted to ensure the azimuth planes intersected.

The pulser settings were 500 Hz PRF and 8 cycles. These settings were limited by the 4 W maximum power output of the DC-DC converters. A 500 Hz PRF was the maximum that could be achieved while maintaining a 400 V steady state amplitude. With these settings the initiation of shock scattering histotripsy was demonstrated starting at the surface and burrowing into the cortex.

Previously with the single channel transducer, a 10 - 15 cycle 450 V pulse with a PRF of 1 kHz was required for a consistent bubble cloud to form. To work around the power limitation, the DC-DC converters were removed and replaced with a bench top high voltage supply. The pulser settings were changed to 12 cycles at a PRF of 1 kHz. The negative supply voltage was increased until reaching a 430 V pulse amplitude, at which point the average power draw from the supply was 7 W. Even with the increased power the transducer was unsuccessful at consistently initiating subcortical cavitation.

Reference [8] states the threshold for initiating a bubble cloud in ex vivo porcine tissue is -13.26 MPa for a PRF 1 kHz, using a 4 cycle 1 MHz frequency pulse. From this it was expected that 306 V would have been enough to cavitate within the rat brain tissue.

A pulse sequence was created to cycle through a + pattern of five foci positioned ±0.75 mm from the nominal focus along the axial and azimuth axis. When positioned just below the surface, distinct cavitation bubble clouds were initiated in sequence at the three azimuthal points along the surface. The bubble cloud then grew to include the point located deeper in the tissue. Fig. 5 shows frames from a video captured during and after treatment. Surface shock scattering resulted in each point growing to a bubble cloud on the order of 0.5 – 1 mm in size. This resulted in the points starting to blur together especially in the axial direction due to the larger axial focal width.

IV. Conclusion

A 16 element histotripsy array was successfully fabricated, characterized, and found to match well with the FEM model. The transducer was able to initiate cavitation extrinsically in water when driven with a 250 V peak-to-peak amplitude pulse.

The results from steering the focus in brain tissue are promising as it shows not only that the array has the potential to cavitate an arbitrary shape, but that it can ablate a much larger region than a single element transducer at the same frequency without the need for mechanical translation.

Acknowledgment

The author would like to thank Thomas Landry for providing the ex vivo tissue samples and his assistance in setting up the ablation experiment.

References

[1] B. C. Tran, Jongbum Seo, T. L. Hall, J. B. Fowlkes and C. A. Cain, "Microbubble-enhanced cavitation for noninvasive ultrasound surgery," in IEEE Transactions on Ultrasonics, Ferroelectrics, and Frequency Control, vol. 50, no. 10, pp. 1296-1304, Oct. 2003.

[2] J. Woodacre, T. Landry and J. Brown, "Real-time imaging, targeting, and ablation of ex-vivo tissue using a handheld histotripsy transducer and coregistered 64-element high-frequency endoscopic phased array," 2016 IEEE International Ultrasonics Symposium (IUS), Tours, 2016, pp. 1-4.

[3] J. K. Woodacre, T. G. Landry and J. A. Brown, "A Low-Cost Miniature Histotripsy Transducer for Precision Tissue Ablation," in IEEE Transactions on Ultrasonics, Ferroelectrics, and Frequency Control, vol. 65, no. 1 1, pp. 2131-2140, Nov. 2018.

[4] J. K. Woodacre, E. Simpson and J. A. Brown, "A 5 mm × 5 mm Square, Aluminum Lens Based Histotripsy Transducer: Reaching the Endoscopic Form Factor," 2018 IEEE International Ultrasonics Symposium (IUS), Kobe, 2018, pp. 1-4.

[5] W. A. Smith and B. A. Auld, "Modeling 1-3 composite piezoelectrics: thickness-mode oscillations," IEEE Transactions on Ultrasonics, Ferroelectrics and Frequency Control, vol. 38, no. 1, pp. 40–47, Jan. 1991.

[6] A. Bezanson, R. Adamson and J. A. Brown, "Fabrication and performance of a miniaturized 64-element high frequency endoscopic phased array," in IEEE Transactions on Ultrasonics, Ferroelectrics, and Frequency Control, vol. 61, no. l, pp. 33-43, January 2014.

[7] J. A. Brown and G. R. Lockwood, "Low-cost, high-performance pulse generator for ultrasound imaging," in IEEE Transactions on Ultrasonics, Ferroelectrics, and Frequency Control, vol. 49, no. 6, pp. 848-851, June 2002.

[8] Eli Vlaisavljevich et. al., "Histotripsy-induced cavitation cloud initiation thresholds in tissues of different mechanical properties," IEEE Trans. Ultrason. Ferroelectr. Freq. Control, vol 61, pp. 341-352, February 2014.